

Articles

Hydrogel-Templated Growth of Large Gold Nanoparticles: Synthesis of Thermally Responsive Hydrogel–Nanoparticle Composites

Jun-Hyun Kim and T. Randall Lee*

Department of Chemistry, University of Houston, 4800 Calhoun Road, Houston, Texas 77204-5003

Received October 4, 2006. In Final Form: March 30, 2007

In this paper, we describe a unique strategy for preparing discrete composite nanoparticles consisting of a large gold core (60–150 nm in diameter) surrounded by a thermally responsive nontoxic hydrogel polymer derived from the polymerization of *N*-isopropylacrylamide (NIPAM) or a mixture of NIPAM and acrylic acid. We synthesize these composite nanoparticles at room temperature by inducing the growth of gold nanoparticles in the presence of preformed spherical hydrogel particles. This new method allows precise control of the size of the encapsulated gold cores (tunable between 60 and 150 nm) and affords composite nanoparticles possessing diameters ranging from as small as 200 nm to as large as 550 nm. Variable-temperature studies show that the hydrodynamic diameter of these composite nanoparticles shrinks dramatically when the temperature is increased above the lower critical solution temperature (LCST); correspondingly, when the temperature is lowered below the LCST, the hydrodynamic diameter expands to its original size. These composite nanoparticles are being targeted for use as optically modulated drug-delivery vehicles that undergo volume changes upon exposure to light absorbed by the gold nanoparticle core.

Introduction

The development of new synthetic routes to nanometer-scale particles continues to be driven by the potential applications offered by their unique optical properties.¹ In particular, research focused on nanoparticle fabrication is urgently needed to develop new nanoscale materials and devices for controlled drug delivery.² Of particular interest is the ability of metal nanoparticles to absorb or scatter light; for many optical applications, nanoparticles are superior to molecular chromophores.³ Research in this area has largely focused on metal nanoparticles (e.g., silver, copper, and gold) because of their ease of fabrication and their strong optical absorbances.^{4–6} Gold nanoparticles have drawn particular attention due to their biocompatibility, which makes them attractive for use in vivo as nanoscale biomaterials.^{7–8}

Colloidal gold nanoparticles are often decorated with organic molecules, inorganic materials, or polymers to facilitate their use in catalysis, photonics, electronics, optics, and biomedicine.^{9–11} While a number of methods have been described for the preparation of polymer-coated gold nanoparticles,^{11–16} these

studies have utilized either polymers that contain strong metal-binding ligands to coordinate to the metal ions and/or nanoparticles or the growth of polymers from the surface of metal nanoparticle cores through covalent attachment or electrostatic interactions. We sought an alternative approach in which the gold nanoparticles are grown within or on a simple hydrogel polymer template. The composite particles of specific interest to us consist of a single gold nanoparticle trapped within a spherical hydrogel polymer matrix. For drug delivery in vivo, these composite nanoparticles should ideally exist as stable dispersed colloids in aqueous solution. Moreover, they should exhibit a rapid swelling–deswelling response to external stimuli,^{7,16} undergoing reversible volume transitions that are strongly dependent on the lower critical solution temperature (LCST) as well as other chemical or physical conditions, such as the solution pH and the nature of the surrounding environment.^{17–19} These and related hydrogel-based materials are being targeted by others for use in a variety of technological applications, including chemical separations, biomedicine, controlled reversible flocculation, the uptake and release of heavy metals, and catalysis.^{20–24}

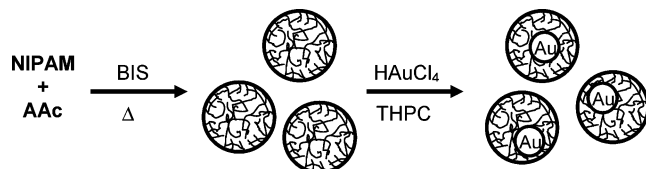
The hydrogels under investigation here are based on homo- and copolymers derived from *N*-isopropylacrylamide (NIPAM) and acrylic acid (AAc), which have been widely studied due to their nontoxic character^{25,26} and thermoresponsive behavior.^{27,28} These hydrogels are hydrophilic and highly soluble in water

* To whom correspondence should be addressed. E-mail: trlee@uh.edu.

- (1) Alivisatos, A. P. *Science* **1996**, *271*, 933.
- (2) Kreibitz, U.; Vollmer, M. *Optical Properties of Metal Clusters*; Springer Series in Material Science 25 (6); Springer: Berlin, 1995.
- (3) Bohren, C. F.; Hoffman, D. R. *Absorption and Scattering of Light by Small Particles*; Wiley: New York, 1998.
- (4) Quanroni, L.; Chumanov, G. *J. Am. Chem. Soc.* **1999**, *121*, 10642.
- (5) Chen, S.; Sommers, J. M. *J. Phys. Chem. B* **2001**, *105*, 8816.
- (6) Clark, H. A.; Campagnok, P. J.; Wuskell, J. P.; Lewis, A.; Loew, L. M. *J. Am. Chem. Soc.* **2000**, *122*, 10234.
- (7) Zhu, M.-Q.; Wang, L.-Q.; Exarhos, G. J.; Li, A. D. Q. *J. Am. Chem. Soc.* **2004**, *126*, 2656.
- (8) O'Neal, D. P.; Hirsch, L. R.; Halas, N. J.; Payne, J. D.; West, J. L. *Cancer Lett.* **2004**, *109*, 171.
- (9) Wang, C.; Flynn, N. T.; Langer, R. *Adv. Mater.* **2004**, *16*, 1074.
- (10) Liz-Marzan, L. M.; Giersig, M.; Mulvaney, P. *Langmuir* **1996**, *12*, 4329.
- (11) Suzuki, D.; Kawaguchi, H. *Langmuir* **2005**, *21*, 8175.
- (12) Kang, Y.; Taton, T. A. *Angew. Chem., Int. Ed.* **2005**, *44*, 409.
- (13) Suzuki, D.; Kawaguchi, H. *Langmuir* **2005**, *21*, 12016.
- (14) Gittins, D. I.; Caruso, F. *J. Phys. Chem. B* **2001**, *105*, 6846.

- (15) Das, M.; Sanson, N.; Fava, D.; Kumacheva, E. *Langmuir* **2007**, *23*, 196.
- (16) Goreliko, I.; Field, L. M.; Kumacheva, E. *J. Am. Chem. Soc.* **2004**, *126*, 15938.
- (17) Schild, H. G.; Tirrell, D. A. *J. Phys. Chem.* **1990**, *94*, 4352.
- (18) Saunders, B. R.; Vincent, B. *J. Chem. Soc., Faraday Trans.* **1996**, *92*, 3385.
- (19) Zhou, S.; Chu, B. *J. Phys. Chem. B* **1998**, *102*, 1364.
- (20) Pelton, R. *Adv. Colloid Interface Sci.* **2000**, *85*, 1.
- (21) Jeong, B.; Bae, Y. H.; Lee, D. S.; Kim, S. W. *Nature* **1997**, *388*, 860.
- (22) Bergbreiter, D. E.; Case, B. L.; Liu, Y. S.; Caraway, J. W. *Macromolecules* **1998**, *31*, 6053.
- (23) Snowden, M. J.; Tomas, D.; Vincent, B. *Analyst* **1993**, *118*, 1367.
- (24) Jones, C. D.; Lyon, L. A. *Macromolecules* **2000**, *33*, 8301.

Scheme 1. Strategy Used To Prepare Gold Nanoparticle–Hydrogel Composites



below their LCST, but become hydrophobic and partially desolvated above their LCST due to the fluctuation of hydrophobic interactions and hydrogen bonding, depending on the details of the polymer structure.²⁹ Pure homopolymer NIPAM hydrogels, however, have limited uses because their thermally modulated conformational change occurs at a fixed LCST of ~ 30 °C.³⁰ Researchers have overcome this limitation by introducing AAc or acrylamide (AAm) into the poly-NIPAM polymer backbone, which can shift the LCST of the copolymer anywhere from 30 to 60 °C.²⁹ These types of hydrogels undergo a completely reversible swelling–deswelling volume transition in response to changes in temperature, leading to their potential use in controlled drug-release applications.^{25,26,32,33}

In the research described here, we prepare spherical homo- or copolymer hydrogel templates using radical polymerization^{34–38} and then grow gold nanoparticles within the hydrogel spheres (see Scheme 1). This strategy is somewhat analogous to that employed by Crooks et al.,³⁹ who use polymeric dendrimers to template the growth of monodisperse small metal nanoparticles (e.g., 1–3 nm) within dendrimer matrixes. Others have also reported the formation of metal nanoparticles (e.g., Cd, Ag, Pd) inside microgel polymers in which multiple metal nanoparticles with small sizes (<10 nm in diameter) are embedded in an individual polymer particle.^{40–42} Our method, in contrast, utilizes hydrogel polymers to template the growth of monodisperse large gold nanoparticles (tunable between 60 and 150 nm) within hydrogel matrixes. Furthermore, our method offers not only tunable gold nanoparticle sizes, but also tunable hydrogel host sizes (tunable between 200 and 550 nm).

Experimental Section

Materials. The monomer NIPAM (Acros, 99%) was recrystallized from hexane and dried under vacuum before use. The comonomer AAc (Acros, 99.5%), cross-linker *N,N'*-methylenebisacrylamide (BIS; Acros, 96%), potassium hydroxide (KOH; EM, 85%), nitric

acid (HNO₃; EM, 70%), ammonium persulfate (APS; EM, 98%), hydrogen tetrachloroaurate(III) hydrate (HAuCl₄·H₂O; 99.9%, Strem), and tetrakis(hydroxymethyl)phosphonium chloride (THPC; Aldrich) were used as received from the indicated suppliers. Water used in all reactions was purified to a resistance of 18 MΩ (Academic Milli-Q Water System, Millipore Corp.) and filtered through a 0.22 μm membrane to remove any impurities. All glassware was cleaned with aqua regia and then with strong base (saturated KOH in isopropyl alcohol) before use.

Gold Nanoparticle Growth Templated by Hydrogels. Hydrogel homopolymer and copolymer nanoparticles ranging from ~ 200 to ~ 550 nm in diameter were prepared by radical polymerization in aqueous solution as described elsewhere.^{24,31} These polymer nanoparticles were used as encapsulating templates to grow gold nanoparticles within the hydrogel particle matrixes. To prepare ~ 550 nm diameter hydrogel particles composed of 95% NIPAM and 5% AAc, NIPAM (1.0 g), AAc (0.05 g), and BIS (0.1 g) were dissolved in 196 mL of purified Milli-Q water and placed in a three-necked round-bottomed flask with an inlet for argon. The solution was purged with argon for 1 h and heated to 70 °C, and then APS (0.4 g/4 mL of water) was added to initiate the polymerization. The reaction was allowed to proceed for 5–6 h. At the end of this period, the solution was filtered through a 1 μm membrane to remove any micrometer-sized impurities and/or any aggregated particles. Homo-NIPAM hydrogel particles (0% AAc) and NIPAM-*co*-AAc hydrogel particles containing 10% AAc, both having ~ 550 nm diameters were prepared similarly. Smaller hydrogel particles (~ 200 nm in diameter) were prepared by increasing the amount of the initiator (APS, 0.64 g/4 mL of water) and the two monomers (NIPAM, 1.425 g; AAc, 0.075 g) but keeping everything else the same.

By analogy to the Duff et al. method for growing gold nanoparticles,^{43,44} we used THPC to reduce gold salts within the preformed hydrogel spheres. In our approach, 50 mL of prepared hydrogel particles was mixed with 1.88 mL of an aqueous solution of 1% HAuCl₄·H₂O, and the mixture was stirred for at least 30 min. Aliquots of 0.33 mL of 1 M NaOH and 1.11 mL of a solution composed of 12 μL of an 80% solution of THPC in 1 mL of water were added simultaneously to the mixture with stirring. The color of the solution changed slowly from colorless to pink, to red, and then to brown over the course of a few minutes depending on the size of the hydrogel particles and/or the proportion of AAc in the hydrogel. The solution was stirred for another 30 min and then centrifuged at 30 °C for 2 h at 3500 rpm. The supernatant was separated to remove any unreacted materials, soluble side products, small gold seed particles formed outside the hydrogel spheres, and pure polymers without gold cores. The purified nanoparticles were then diluted with pure Milli-Q water and stored at room temperature for later use. The size of the gold–hydrogel composite particles was similar to that of the pristine unimpregnated hydrogel nanoparticles. Adjusting the initial amounts of gold salt, NaOH, and THPC afforded ready control over the size of the gold cores.

Characterization Methods. To characterize the composition, morphology, optical properties, and hydrodynamic diameters of the hydrogel templates, gold nanoparticles, and gold–hydrogel composite nanoparticles, we used a combination of field emission scanning electron microscopy (FE-SEM), transmission electron microscopy (TEM), ultraviolet–visible (UV–vis) spectroscopy, and dynamic light scattering (DLS). Due to our interest in large hydrogel templates for maximal drug loading and transport, our most thorough analyses were focused on the largest composite particles reliably formed via this method (i.e., using NIPAM homopolymer templates).

We used a Cary 50 scan UV–vis optical spectrometer (Varian) equipped with Cary Win UV software to evaluate the optical properties of the gold nanoparticles and hydrogel-coated gold nanoparticles. UV–vis spectra of the gold nanoparticles were collected by diluting the particles with water, transferring them to an optical quartz cell, and scanning over a range of wavelengths (300–1100 nm).

- (25) Gutowska, A.; Bae, Y. H.; Jacobs, H.; Mohammad, F.; Mix, D.; Feijen, J.; Kim, S. W. *J. Biomed. Mater. Res.* **1995**, *29*, 811.
 (26) Matsumaru, Y.; Hyodo, A.; Nose, T.; Ito, S.; Hirano, T.; Ohashi, S. *J. Biomater. Sci., Polym. Ed.* **1996**, *7*, 795.
 (27) Jones, C. D.; Lyon, L. A. *Macromolecules* **2003**, *36*, 1988.
 (28) Mears, S. J.; Deng, Y.; Cosgrove, T.; Pelton, R. *Langmuir* **1997**, *13*, 1901.
 (29) Winnik, F. M. *Polymer* **1990**, *31*, 2125.
 (30) Pelton, R. H.; Pelton, H. M.; Morphis, A.; Rowell, R. L. *Langmuir* **1989**, *5*, 816.
 (31) Snowden, M. J.; Chowdhry, B. Z.; Vincent, B.; Morris, G. E. *J. Chem. Soc., Faraday Trans.* **1996**, *92*, 5013.
 (32) Serksen, S. R.; Westcott, S. L.; Halas, N. J.; West, J. L. *J. Biomed. Mater. Res.* **2000**, *51*, 293.
 (33) Hu, Z.; Xia, X. *Adv. Mater.* **2004**, *16*, 305.
 (34) Saunders, B. R.; Vincent, B. *Adv. Colloid Interface Sci.* **1999**, *80*, 1.
 (35) Saunders, B. R.; Crowther, H. M.; Vincent, B. *Macromolecules* **1997**, *30*, 482.
 (36) Neyret, S.; Vincent, B. *Polymer* **1997**, *38*, 6129.
 (37) Kim, J.-H.; Lee, T. R. *Chem. Mater.* **2004**, *16*, 3647.
 (38) Kim, J.-H.; Lee, T. R. *Drug Dev. Res.* **2006**, *67*, 4120.
 (39) For a particularly relevant example, see: Knecht, M. R.; Garcia-Martinez, J. C.; Crooks, R. M. *Langmuir* **2005**, *21*, 11981.
 (40) Xu, S.; Zhang, J.; Paquet, C.; Lin, Y.; Kumacheva, E. *Adv. Funct. Mater.* **2003**, *13*, 468.
 (41) Mei, Y.; Lu, Y.; Polzer, F.; Ballauff, M. *Chem. Mater.* **2007**, *19*, 1062.
 (42) Lu, Y.; Mei, Y.; Drechsler, M.; Ballauff, M. *Angew. Chem., Int. Ed.* **2006**, *45*, 813.

(43) Duff, D. G.; Baiker, A.; Edwards, P. P. *Langmuir* **1993**, *9*, 2301.

(44) Duff, D. G.; Baiker, A.; Gameson, I.; Edwards, P. P. *Langmuir* **1993**, *9*, 2310.

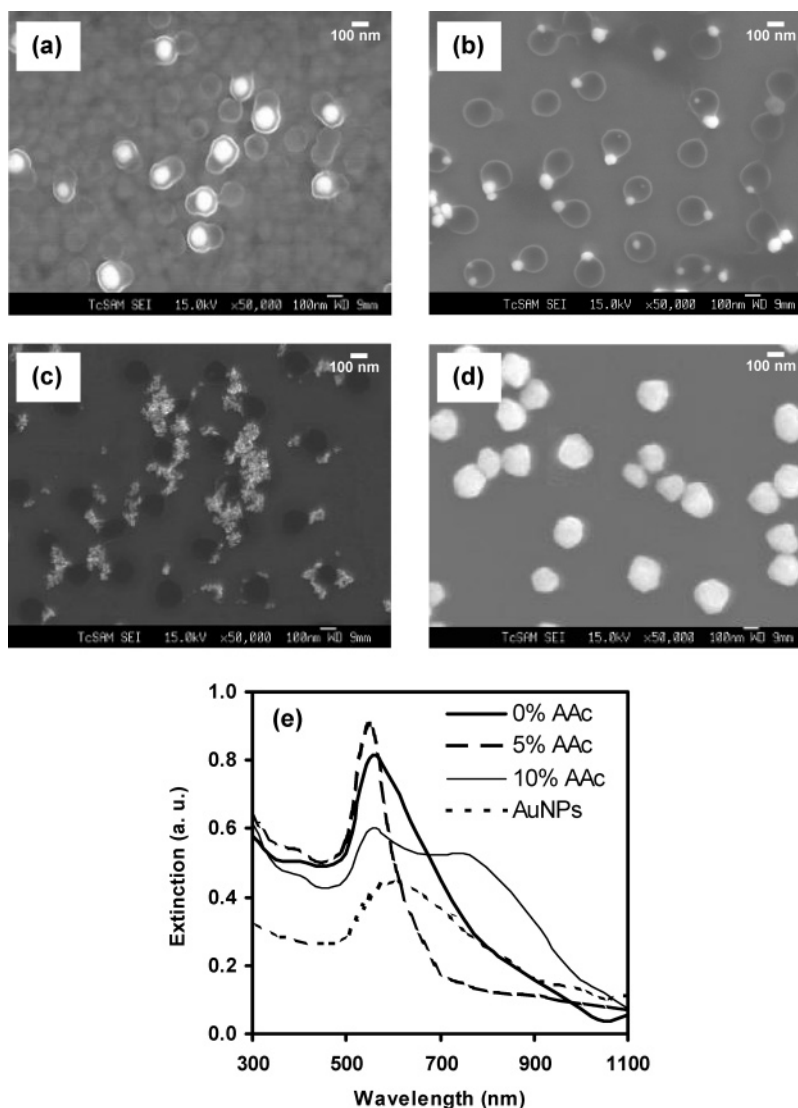


Figure 1. Gold nanoparticles templated from hydrogel particles ~ 200 nm in diameter. FE-SEM images of samples templated from (a) 100% NIPAM and 0% AAc, (b) 95% NIPAM and 5% AAc, (c) 90% NIPAM and 10% AAc, and (d) 100% NIPAM and half the amount of reducing agent. (e) UV-vis spectra of samples a–d. Scale bar 100 nm.

Morphology studies and elemental analysis by FE-SEM were performed using a JSM 6330F (JEOL) instrument operating at 15 kV. For the FE-SEM images, the gold nanoparticles and gold–hydrogel composite nanoparticles were deposited on Formvar-coated copper grids and completely dried at room temperature overnight before analysis. The samples were then coated with a carbon film (25 nm in thickness) using a carbon sputterer under vacuum. Analysis by FE-SEM demonstrated the overall morphological uniformity of the particles (*vide infra*).

For analyses by TEM, we used a JEM-2000 FX electron microscope (JEOL) operating at an accelerating voltage of 200 kV. All of the samples for TEM were deposited on 300 mesh holey carbon-coated copper grids and then dried before analysis. Due to the low electron density of the hydrogels, the gold–hydrogel composite nanoparticles were mixed with negative staining (e.g., 1% uranyl acetate dihydrate)²⁴ to enhance visualization.

For the DLS measurements, an ALV-5000 multiple- τ digital correlation instrument operating at a light source wavelength of 514.5 nm and a fixed scattering angle of 90° was used to measure the hydrodynamic diameters as a function of temperature for bare gold nanoparticles and hydrogel-coated gold nanoparticles. The samples were measured at dilute concentrations with precise control over the temperature to reduce artifacts arising from convection currents in the samples.

Results and Discussion

We explored the strategy of growing gold nanoparticles in the presence of NIPAM-based hydrogel polymers because we believed that these hydrogels, by analogy to PAMAM dendrimers,³⁹ might serve as hosts to template the growth of gold nanoparticles. Figure 1 shows the FE-SEM images of gold–hydrogel composite nanoparticles (~ 200 nm in diameter) obtained from gold nanoparticle growth on or within various NIPAM hydrogel polymers. The observed preference for surface localization of the gold nanoparticles probably arises from diffusion-based phenomena; alternatively, growth of the gold nanoparticles within the hydrogel particles will disrupt a greater number of interchain hydrogen bonds than will growth at the surface. We note that gold nanoparticle–hydrogel composites having little or no AAc content (i.e., 0% AAc and 5% AAc, parts a and b, respectively, of Figure 1) were prepared more reliably than those having 10% AAc content, which tended to form aggregates of small gold nanoparticles on the outside of the hydrogel particles under our reaction conditions (Figure 1c). In addition, the TEM images also show that the gold–hydrogel composite nanoparticles comprised of 0% and 5% AAc contained a few pristine hydrogel nanoparticles having no gold core. Although the diameters of all

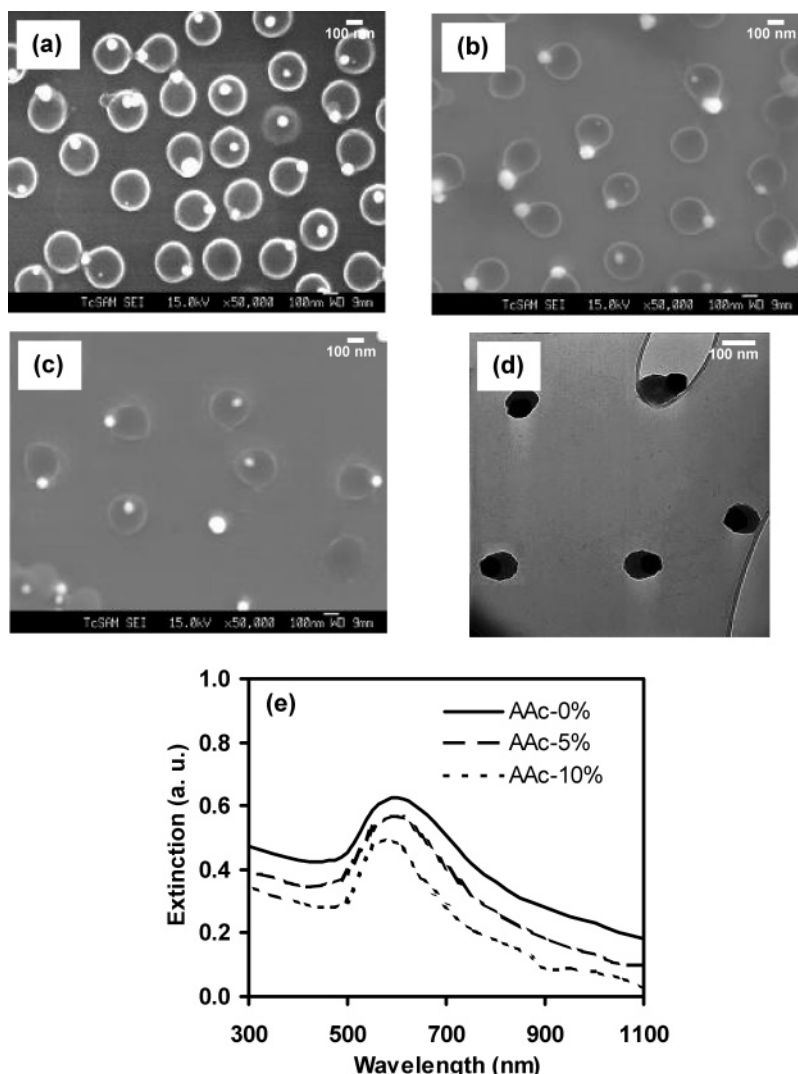


Figure 2. Gold nanoparticles templated from hydrogel particles ~ 550 nm in diameter. FE-SEM images of samples templated from (a) 100% NIPAM and 0% AAc, (b) 95% NIPAM and 5% AAc, and (c) 90% NIPAM and 10% AAc. (d) TEM image of sample b. (e) UV-vis spectra of samples a–c. Scale bar 100 nm.

hydrogel templates examined in these experiments were about the same, the gold nanoparticle cores grew largest when using the hydrogel homopolymer template (0% AAc) compared to those obtained when using the two hydrogel copolymer templates (5% AAc and 10% AAc). It is possible that the increased number of AAc groups along the polymer backbone leads to increased interchain hydrogen bonding and thus decreased chain mobility and interchain separation, which can plausibly inhibit the growth of gold nanoparticles within the hydrogel particles.⁴⁵ Alternatively, given that the surfaces of gold nanoparticles are negatively charged,⁴⁶ the contrasting behavior of the templates can perhaps be attributed to the partial inhibition of gold nanoparticle nucleation by the negatively charged AAc moieties in the copolymer templates.

The synthetic approach described here also allows the facile preparation of large gold nanoparticles having undetectably thin hydrogel coatings. Specifically, by using ~ 200 nm NIPAM particles as templates and decreasing the amount of reducing agent (THPC), we were able to grow large gold nanoparticles having diameters ranging from 60 nm to more than 150 nm (Figure 1d). Importantly, these large gold nanoparticles were

remarkably stable (i.e., no aggregation and no changes in the optical properties) over 3 months at room temperature as analyzed by UV-vis and FE-SEM. While the observed stability is consistent with the presence of a polymeric stabilizer on the gold nanoparticle surfaces, we could detect no such species by FE-SEM, TEM, or DLS. In separate experiments, we rarely observed the formation of large gold nanoparticles when using hydrogel templates ~ 550 nm in diameter (vide infra) or no hydrogel templates at all.

The UV-vis spectra in Figure 1e show peaks at $\lambda \approx 530$ –600 nm, which are characteristic of Au nanoparticles.^{47–49} Interestingly, the Au nanoparticles templated by the pure NIPAM polymer exhibit a slightly longer absorption wavelength than those templated by the 5% AAc polymer, which suggests the formation of slightly larger gold nanoparticles for the former template.⁵⁰ The spectrum of the gold nanoparticles templated by the 10% AAc polymer shows two distinct peaks, which we assign to the presence of small gold nanoparticles ($\lambda \approx 530$ nm) and aggregates

(47) Link, S.; El-Sayed, M. A. *J. Phys. Chem. B* **1999**, *103*, 4212.

(48) Frens, G. *Nat. Phys. Sci.* **1973**, *241*, 20.

(49) Liu, F.-K.; Hsieh, S.-Y.; Ko, F.-H.; Chu, T.-C.; Dai, B.-T. *Jpn. J. Appl. Phys.* **2003**, *42*, 4147.

(50) Turkevich, J.; Stevenson, P. C.; Hillier, J. *Discuss. Faraday Soc.* **1951**, *58*, 55.

(45) Morris, G. E.; Vincent, B.; Snowden, M. J. *J. Colloid Interface Sci.* **1997**, *190*, 198.

(46) Vogel, W.; Duff, D. G.; Baiker, A. *Langmuir* **1995**, *11*, 401.

of gold nanoparticles ($\lambda \approx 750$ nm).^{47–51} As noted above, the FE-SEM images in Figure 1c provide complementary support for the formation of the latter aggregates. We also note that the gold nanoparticles shown in Figure 1d show one broad absorption peak at $\lambda \approx 600$ nm, which is consistent with the presence of large Au nanoparticles having diameters greater than 100 nm.^{48–50}

Figure 2 shows the FE-SEM, TEM, and UV-vis spectra of gold-hydrogel composite nanoparticles prepared from hydrogel templates having diameters of ~ 550 nm. All images show that the size of the hydrogel templates remains constant as prepared (i.e., growth of the gold nanoparticle exerts no major influence on the original hydrogel particle diameter). Consistent with our observations above with the smaller templates, the diameters of these large hydrogel particles decrease slightly with increasing AAc content (as measured by the DLS). In particular, gold nanoparticles templated with the NIPAM homopolymers were noticeably larger than those templated with the copolymers. Furthermore, products from the latter reactions required multiple purification cycles due to the production of a mixture of composite particles and free gold nanoparticles as shown in Figure 2c. For these large composites (~ 550 nm in diameter), the enhanced template effect observed for the homopolymer particles (0% AAc) compared to that of the two copolymer particles (5% AAc and 10% AAc) likely arises from the same phenomena affecting the smaller hydrogel composites (~ 200 nm in diameter, vide supra).

We note that the TEM image in Figure 2d shows somewhat shrunken hydrogels when compared to those in the FE-SEM image in Figure 2c. This difference probably arises from the ultrahigh vacuum and electron beam used in the TEM analyses; both can plausibly lead to dehydration of the hydrogel polymer matrix. This hypothesis is supported by vacuum experiments highlighted below and by our general observation that the composite nanoparticle diameters measured by DLS were closer in magnitude to the diameters estimated from the FE-SEM images than those estimated from the TEM images.

From the UV-vis spectra in Figure 2e, the peak assigned to the $\text{HAuCl}_4 \cdot \text{H}_2\text{O}$ salt solution at $\lambda \approx 300\text{--}350$ nm completely disappears upon reduction, and peaks at $\lambda \approx 550\text{--}570$ nm appear—observations that are characteristic of gold nanoparticle formation.⁵⁰ We also observed that the gold nanoparticles templated by the hydrogel homopolymer particles exhibit a slightly longer absorption wavelength than those templated by the copolymers, which suggests the formation of slightly larger gold nanoparticles in the former system.⁵⁰ This observation is consistent with the analyses by FE-SEM and TEM (vide supra).

Figure 3 again shows hydrogel-gold nanoparticles grown with the large hydrogel templates (~ 550 nm). Comparison of Figure 3a with Figure 3b after treatment at 30°C under vacuum (68 kPa) for 24 h shows a significant decrease in size (from ~ 550 nm to ~ 350 nm in diameter), consistent with dehydration of the hydrogel matrix as postulated above for samples subjected to analysis by TEM. Most of the particles in Figure 3b appear as a light halo surrounding a dark core (in addition to a small bright gold particle). Apparently, dehydration of the hydrogel leads to shrinkage of the particle, which is accompanied by pinning of the particle edges to the substrate surface. In other words, as the particles dry and retract across the surface, a thin layer of polymer is left behind, appearing as a halo around the periphery of each shrunken polymer core. The diameter of the dark core is ~ 300 nm, which is nearly identical to the value measured by DLS of the particles heated to 30°C in solution (vide infra). It

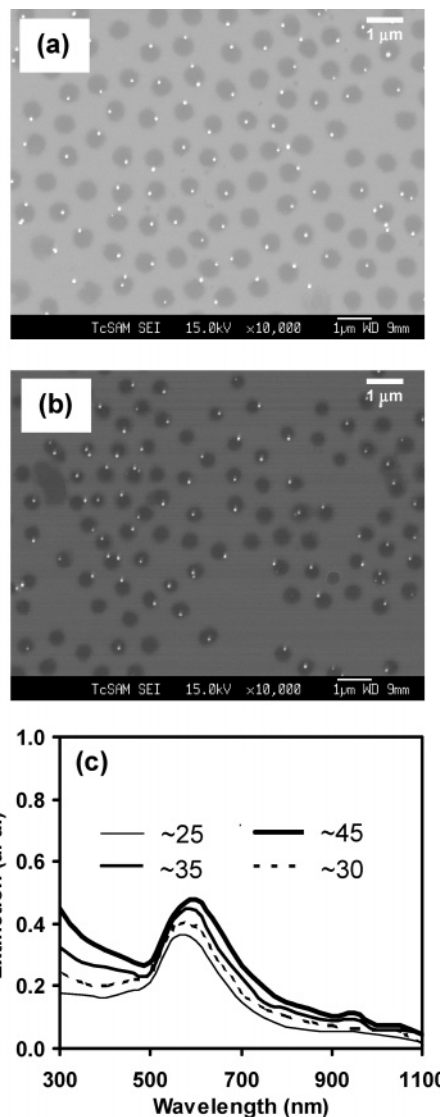


Figure 3. Gold nanoparticle-hydrogel composites templated from the NIPAM homopolymer (~ 550 nm). FE-SEM images of samples (a) freshly prepared and (b) held at 68 kPa and 30°C for 24 h. (c) UV-vis spectra as a function of cycling from 25 to 35 to 45°C and then to 30°C . Scale bar $1\ \mu\text{m}$.

is also possible that the dehydrated particle in Figure 3b has flattened on the surface and thus appears larger than its true average diameter.

UV-vis spectra of these samples as a function of temperature (Figure 3c) show that the absorption intensity increases slightly as the temperature is raised above the LCST and the absorbance maximum shifts to slightly longer wavelength. Upon cooling of the sample back to the LCST, the spectrum returns to its original appearance, consistent with the deswelling-swelling behavior of the hydrogel matrix (vide infra).⁷ Above the LCST, the collapsed hydrogel matrix gives rise to enhanced scattering due to an increase in the local refractive index surrounding the gold nanoparticles as described by Mie theory.⁵² At or below the LCST, the hydrogel matrix is swollen due to hydrogen bonding between water molecules and the amide moieties in the hydrogel.^{7,45,53} The results here support the strong association of the hydrogel matrix with the nanoparticle guest.

We also monitored the hydrodynamic diameters of the hydrogel-gold nanoparticle composites as a function of tem-

(51) Oldenburg, S. J. Ph.D. Thesis, Department of Electrical Engineering, Rice University, Houston, TX, 1999.

(52) Mie, G. *Ann. Phys. (Leipzig)* **1908**, 25, 377.

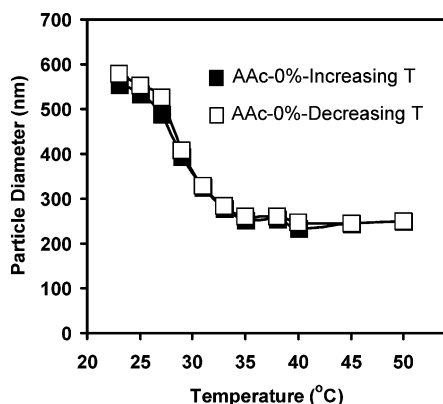


Figure 4. Hydrodynamic diameter as a function of temperature of gold nanoparticle–hydrogel composites grown from NIPAM homopolymers. Filled symbols correspond to increasing T ; open symbols correspond to decreasing T .

perature. Figure 4 shows that, as the temperature was increased above 26 °C, the gold–NIPAM particle diameters decreased gradually and became constant at temperatures above 40 °C. The changes in diameter of the NIPAM homopolymer composite occurred at a lower temperature (~30 °C) than those derived from the 5% AAc copolymer (~40 °C, data not shown). This difference can be attributed to the presence of ionized carboxylate groups in the latter hydrogel, which can greatly influence temperature-induced conformational changes.³¹ The lower LCST and rapid volume transitions in a narrow range of temperature are consistent with literature observations.^{31,53,54} This behavior is reversible, reflecting the deswelling–collapsing behavior of the hydrogel matrix. Collapse of the hydrogel at elevated temperatures arises from the loss of hydrogen bonding to amide groups (hydrophilic sites of $-C=O$ and $-NH$) in the hydrogel copolymer.⁵⁵ The thermally induced loss of hydrogen bonding within the hydrogel polymer matrix eliminates internal electrostatic repulsive forces, leading to a collapse of the expanded structure.⁷ Thus, the presence of water molecules and hydrophilic sites in the polymer backbone provides hydrogen-bonding interactions at low temperatures, allowing electrostatic repulsion to give the water-swelling property.⁵⁶ A small reduction in the percent volume change for the gold–NIPAM composite particles when compared to simple NIPAM particles can be attributed to the invariant diameter of the gold nanoparticles. Nevertheless, the observation of large volume changes for these composite nanoparticles is consistent with their targeted use as drug-delivery vehicles. Future studies will explore drug impregnation/release and optical heating, with a particular emphasis on near-IR activation.^{7,32}

In previous studies,^{37,38} we prepared gold nanoparticles coated with typically thinner hydrogel overlayers (composite diameter

≤ 250 nm) by growing hydrogel polymers from the surface of 60 nm gold nanoparticle templates; moreover, for these first-generation composites, the gold nanoparticles appeared centrally located within the hydrogel spheres. In contrast, the new inverse synthetic strategy reported here produces gold–hydrogel composites having substantially greater dimensions (up to ~550 nm) and where the gold nanoparticles are either centrally located or more typically located on or near the perimeter of the hydrogel sphere. As noted above, larger host sizes offer enhanced drug-loading capacity—one of the long-term goals of our research. An additional benefit offered by our new method is the ability to prepare large gold nanoparticles (with diameters tunable between 60 and 150 nm) that are stable against aggregation in aqueous solution for more than 3 months.

A remaining issue centers on the possible mechanism(s) by which the NIPAM-based hydrogels exert their unique template effect. Given that (1) the uncharged NIPAM homopolymer particles perform better as templates than the negatively charged AAc-containing copolymer particles, (2) the growing nanoparticles bear a net negative charge due to capping by $AuCl_2^-$ species,⁴⁶ and (3) the partial charge on the reducing hydride is negative, we propose that the relatively labile hydrogen on the amide nitrogen of poly-NIPAM, $-NH(CO)-$, promotes partial Au nanoparticle neutralization through hydrogen-bond formation with the nanoparticle surface during the reduction. This partial neutralization (or charge stabilization) serves to lower the barrier to reduction of Au(I) to Au(0).

Conclusions

The studies reported here demonstrate an effective strategy for preparing discrete gold–hydrogel composite nanoparticles. Analyses by FE-SEM, TEM, UV–vis, and DLS collectively support the formation and isolation of the composite nanoparticles, which showed reversible phase transitions (deswelling–swelling) in aqueous solution with increasing and decreasing temperature, respectively. The overall dimensions of the composite nanoparticles could be varied from ~200 to ~550 nm, and the diameters of the gold nanoparticle cores could be varied from ~60 to ~150 nm. The approach reported here represents a unique method for producing gold–hydrogel composites and colloiddally stable large gold nanoparticles. Furthermore, the ability to modulate the nanoparticle diameters at or near physiologic temperatures renders these nanoparticles attractive candidates for nanoscale drug-delivery applications.

Acknowledgment. We gratefully acknowledge financial support from the Army Research Office, the National Science Foundation (Grant ECS-0404308), the Texas Center for Superconductivity, and the Robert A. Welch Foundation (Grant E-1320). We also thank Dr. J. K. Meen for assistance with the FE-SEM measurements and Dr. I. Rusakova for assistance with the TEM measurements. Use of the DLS device was made possible by a grant from the Department of Energy to Professor Simon Moss (University of Houston).

LA0629173

(53) Tan, K. C.; Wu, X. Y.; Pelton, R. H. *Polymer* **1992**, *33*, 436.

(54) Tan, K. C.; Ragaram, S.; Pelton, R. H. *Langmuir* **1994**, *10*, 418.

(55) Shibayama, M.; Mizutani, S.; Nomura, S. *Macromolecules* **1996**, *29*, 2019.

(56) Kato, E. *J. Chem. Phys.* **1997**, *106*, 3792.